arXiv:0810.3579v1 [cs.CV] 20 Oct 2008

Hierarchical bag of paths for kernel based shape classification

François-Xavier Dupé* and Luc Brun

GREYC UMR CNRS 6072,
ENSICAEN-Université de Caen Basse-Normandie,
14050 Caen France,
{francois-xavier.dupe,luc.brun}@greyc.ensicaen.fr

Abstract. Graph kernels methods are based on an implicit embedding of graphs within a vector space of large dimension. This implicit embedding allows to apply to graphs methods which where until recently solely reserved to numerical data. Within the shape classification framework, graphs are often produced by a skeletonization step which is sensitive to noise. We propose in this paper to integrate the robustness to structural noise by using a kernel based on a bag of path where each path is associated to a hierarchy encoding successive simplifications of the path. Several experiments prove the robustness and the flexibility of our approach compared to alternative shape classification methods.

Key words: Shape, Skeleton, Support Vector Machine, Graph Kernel

1 Introduction

The skeleton of a $2D$ shape is defined as the location of the singularities of the signed distance function to the border of the shape. This structure has several interesting properties: it is thin, homotopic to the shape, invariant under rigid transformations of the plane and most importantly it has a natural interpretation as a graph. The representation of a shape by a skeletal (or shock) graph has become popular owing the good properties of this representation inherited from the properties of the skeleton. However, beside all this good properties, the skeletonization is not continuous and small perturbations of the boundary insert structural noise within the graph encoding the shape.

Several graph based methods have been proposed to compute a distance between shapes robust to such a structural noise. Sharvit et al. [1] propose a graph matching method based on a graduated assignment algorithm. Siddiqi [2] proposes to transform the shock graph into a tree and then applies a tree matching algorithm. Pellilo [3] uses the same tree representation but transforms the tree matching problem into a maximal clique problem within a specific association graph.

* This work is performed in close collaboration with the laboratory Cycéron and is supported by the CNRS and the région Basse-Normandie.

All the above graph methods operate directly on the space of graphs which contains almost no mathematical structure. This lack of mathematical structure forbids the use of basic statistical tools such as the mean or the variance. Graph kernels provide an elegant solution to this problem. Using appropriate kernels, graphs can be mapped either explicitly or implicitly into a vector space whose dot product corresponds to the kernel function. All the "natural" operations on a set of graphs which were not defined in the original graph space are now possible into this transformed vector space. In particular, graph kernels may be combined with the kernelised version of robust classification algorithms such as the Support Vector Machine (SVM).

A Graph kernel used within the shape representation framework should take into account the structural noise induced by the skeletonization process. Bunke [4] proposes to combine edit distance and graph kernels by using a set of n prototype graphs $\{g_1, \ldots, g_n\}$. Given a graph edit distance $d(.,.)$, Bunke associates to each graph g the vector $\phi(g) = (d(g, g_1) \ldots, d(g, g_n))$. The kernel $k(g_1, g_2)$ between the two graphs g_1 and g_2 is then defined as the dot product $< \phi(g_1), \phi(g_2) >$.

Neuhaus [5] proposes a similar idea by defining for a prototype graph g_0, the kernel: $k_{g_0}(g, g') = \frac{1}{2}\left(d^2(g, g_0) + d^2(g_0, g') - d^2(g, g')\right)$, where $d(.,.)$ denotes the graph edit distance. Several graph prototypes may be incorporated by summing or multiplying such kernels. Using both Neuhaus [5] and Bunke [4] kernels two close graphs should have close edit distance to the different graph prototypes. The metric induced by such graph kernels is thus relative both to the weights used to define the edit distance and to the graph prototypes. This explicit use of prototype graphs may appear as artificial in some application. Moreover, the definite positive property of these kernels may not in general be guaranteed.

Suard [6] proposes to use the notion of bag of paths of finite length for shape matching. This method associates to each graph all its paths whose length is lower than a given threshold. The basic idea of this approach is that two close shapes should share a large amount of paths. A kernel between these sets should thus reflect this proximity. However, small perturbations may drastically reduce the number of common paths between two shapes (Section 3.2). Moreover, the straightforward definition of a kernel between set of paths does not lead to a definite positive kernel (Section 2.1).

This paper proposes a new definite positive kernel between set of paths which takes into account the structural noise induced by the skeletonization process. We first present in Section 2 the bag of paths approach for shape similarity. Our contributions to this field are then presented in Section 3. The effectiveness of our method is demonstrated through experiments in Section 4.

2 Kernels on bag of paths

Let us consider a graph $G = (V, E)$ where V denotes the set of vertices and $E \subset V \times V$ the set of edges. As mentioned in Section 1 a bag of paths P of length s associated to G contains all the paths of G of length lower than s. We

denote by $|P|$ the number of paths inside P. Let us denote by K_{path} a generic kernel between paths. Given two graphs G_1 and G_2 and two paths $h_1 \in P_1$ and $h_2 \in P_2$ of respectively G_1 and G_2, $K_{path}(h_1, h_2)$ may be interpreted as a measure of similarity between h_1 and h_2 and thus as a local measure of similarity between these two graphs. The aim of a kernel between bags of paths consits to agregate all these local measures between pairs of paths into a global similarity measure between the two graphs.

2.1 The max kernel

This first method, proposed by Suard [6], uses the kernel K_{path} as a measure of similarity and computes for each path $h_1 \in P_1$ the similarity with its closest path in $P_2(\max_{h_j \in P_2} \ K_{path}(h_1, h_j))$. A first global measure of similarity between P_1 and P_2 is then defined as:

$$\hat{K}_{max}(G_1, G_2) = \hat{K}_{max}(P_1, P_2) = \frac{1}{|P_1|} \sum_{h_i \in P_1} \max_{h_j \in P_2} K_{path}(h_i, h_j). \tag{1}$$

The function $\hat{K}_{max}(G_1, G_2)$ is however not symmetric according to G_1 and G_2. Suard obtains a symmetric function interpreted as a graph kernel by taking the mean of $\hat{K}_{max}(G_1, G_2)$ and $\hat{K}_{max}(G_2, G_1)$:

$$K_{max}(G_1, G_2) = \tfrac{1}{2} \left[\hat{K}_{max}(G_1, G_2) + \hat{K}_{max}(G_2, G_1) \right]. \tag{2}$$

This kernel is not positive definite in general. However as shown by Haasdonk [7], SVM with indefinite kernels have in some cases a geometrical interpretation as the maximization of distances between convex hulls. Moreover, experiments (section 4, and [6]) show that this kernel usually leads to valuable results.

2.2 The matching kernel

The non definite positiveness of the kernel K_{max} is mainly due to the max operator. Suard [6] proposes to replace the kernel K_{path} by a kernel which decreases abruptly when the two paths are different. The resulting kernel is defined as:

$$K_{matching}(G_1, G_2) = K_{matching}(P_1, P_2) = \frac{1}{|P_1|} \frac{1}{|P_2|} \sum_{h_i \in P_1} \sum_{h_j \in P_2} \exp\left(\frac{-d^2_{path}(h_i, h_j)}{2\sigma^2} \right). \tag{3}$$

where d_{path} is the distance associated to the kernel K_{path} and defined by: $d^2_{path}(h_1, h_2) = K_{path}(h_1, h_1) + K_{path}(h_2, h_2) - 2K_{path}(h_1, h_2)$.

The resulting function defines a definite positive kernel. This kernel relies on the assumption that using a small value of σ, the couple of paths with the smallest distance will predominate the others in equation 3. This kernel may thus lead to erroneous results if the distance are of the same order of magnitude than σ or if several couples of paths have nearly similar distances.

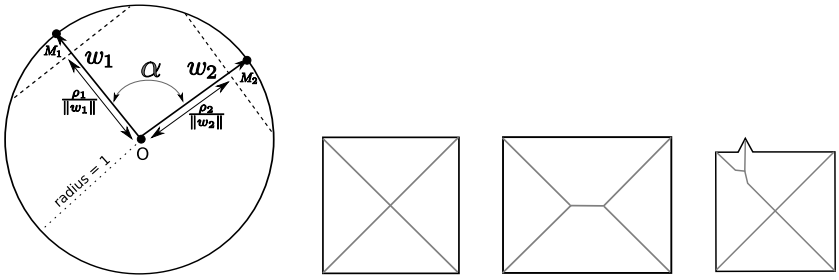

(a) Sets on the unit sphere (b) original (c) edge protrusion (d) node insertion

Fig. 1. Separating two sets using one-class SVM (a). The symbols (w_1, ρ_1) and (w_2, ρ_2) denote the parameters of the two hyperplanes which are represented by dashed lines. Influence of small perturbations on the bag of paths ((b), (c) and (d))

2.3 The change detection kernel

Desobry [8] proposed a general approach for the comparison of two sets which has straightforward applications in the design of a kernel between bags (sets) of paths. Desobry models the two sets as the observation of two sets of random variables in a feature space and proposes to estimate a distance between the two distributions without explicitly building the pdf of the two sets.

The feature space considered by Desobry is based on the normalised kernel $(K(h,h') = K_{path}(h,h')/\sqrt{(K_{path}(h,h)K_{path}(h',h'))})$. Using such a kernel we have $\|h\|_K^2 = K(h,h) = 1$ for any path. The image in the feature space of our set of paths lies thus on an hypersphere of radius 1 centered at the origin (Fig. 1). Desobry defines a region on this sphere by using a single class ν-SVM. This region corresponds to the density support estimate of the unknown pdf of the set of paths [8].

Using Desobry's method, two set of vectors are thus map onto two regions of the unit sphere and the distance between the two regions corresponds to a distance between the two sets. Several kernels based on this mapping have been proposed:

1. Desobry proposed [8] to define the distance between the two spherical arcs as a contrast measure defined by: $d^2_{Desobry}(P_1,P_2) = \frac{\arccos\left(\frac{w_1 K_{1,2} w_2}{\|w_1\|\|w_2\|}\right)}{\arccos\left(\frac{\rho_1}{\|w_1\|}\right)+\arccos\left(\frac{\rho_2}{\|w_2\|}\right)}$.
   This distance is connected to the Fisher ratio (see [8, Section IV]). However, the definite positiveness of the Gaussian RBF kernel based on this distance remains to be shown.
2. Suard [6] proposed the following kernel: $K_{Suard}(G_1,G_2) = K_{Suard}(P_1,P_2) = \rho_1\rho_2 \sum_{h_i\in P_1}\sum_{h_j\in P_2} \alpha_{1,i}\ K_{path}(h_i,h_j)\alpha_{2,j}$ with $w_1 = (\alpha_{1,1},\ldots,\alpha_{1,|P_1|})$ and $w_2 = (\alpha_{2,1},\ldots,\alpha_{2,|P_2|})$.
   This kernel is definite positive, but does not correspond to any straightforward geometric interpretation.

2.4 Path kernel

All the kernels between bags of paths defined in Section 2 are based on a generic kernel K_{path} between paths. A kernel between two paths $h_1 = (v_1, \ldots, v_n)$ and $h' = (v'_1, \ldots, v'_p)$ is classically [9] built by considering each path as a sequence of nodes and a sequence of edges. This kernel denoted $K_{classic}$ is then defined as 0 if both paths have not the same size and as follows otherwise:

$$K_{classic}(h, h') = K_v(\varphi(v_1), \varphi(v'_1)) \prod_{i=2}^{|h|} K_e(\psi(e_{v_{i-1}v_i}), \psi(e_{v'_{i-1}v'_i})) K_v(\varphi(v_i), \varphi(v'_i)) \tag{4}$$

where $\varphi(v)$ and $\psi(e)$ denote respectively the vectors of features associated to the node v and the edge e. The terms K_v and K_e denote two kernels between respectively nodes and edge's features. For the sake of simplicity, we have used Gaussian RBF kernels between the attributes of nodes and edges (Section 4).

3 Hierarchical kernels

Since the main focus of this paper is a new kernel method for shape classification, the construction of skeletal graphs from shapes has been adressed using classical methods. We first build a skeleton using the method proposed by Siddiqi [2]. However the graph we build from the skeleton does not correspond to the shock graph proposed by Siddiqi. Indeed, this graph provides a precise description of the shape but remains sensitive to small perturbations of the boundary. We rather use the construction scheme proposed by Suard [6] and Ruberto [10] which consists to select as node all the pixels of the skeleton which correspond to end points or junctions. These nodes are then connected by edges, each edge being associated to one branch of the skeleton. Given a skeletal graph G we valuate each of its edge by an additive weight measure and we consider the maximal spanning tree T of G. The bag of path associated to G is built on the tree T. Note that, the skeletonization being homotopic we have $G = T$ if the $2D$ shape does not contain any hole.

3.1 Bag of path kernel

None of the bag of path kernels proposed by Desobry or Suard (Section 2) is both definite positive and provides a clear geometrical interpretation. We thus propose a new kernel based on the following distance:

$$d^2_{change}(P_1, P_2) = \arccos\left(\frac{w_1 K_{1,2} w_2}{\|w_1\| \, \|w_2\|}\right). \tag{5}$$

This distance corresponds to the angle α between the two mean vectors w_1 and w_2 of each region (Fig. 1). Such an angle may be interpreted as the geodesic

distance between two points on the sphere and has thus a clear geometrical interpretation. Based on this distance we use the Gaussian RBF kernel:

$$K_{change}(G_1, G_2) = K_{change}(P_1, P_2) = \exp\left(\frac{-d^2_{change}(P_1, P_2)}{2\sigma^2}\right). \quad (6)$$

This kernel is definite positive since the normalized scalar product is positive definite and arccos is bijective on $[0, 1]$. The Gaussian RBF kernel based on this distance is thus definite positive (see [11] for further details).

3.2 Hierarchical kernel between paths

A mentioned in Section 1, the use of kernels between bags of paths within the shape matching framework relies on the assumption that the graphs associated to two similar shapes share a large amount of similar paths. This assumption is partially false since a small amount of structural noise may have important consequences on the set of paths. Let us for example, consider the small deformation of the square (Fig. 1(b)) represented on Fig. 1(c). This small deformation transforms the central node in Fig. 1(b) into an edge (Fig. 1(c)). Consequently graphs associated to these two shapes only share two paths of length 2 (the ones which connect the two corners on the left and right sides). In the same way, a small perturbation of the boundary of the shape may add branches to the skeleton(Fig. 1(d)). Such additional branches i) split existing edges into two sub edges by adding a node and ii) increase the size of the bag of path either by adding new paths or by adding edges within existing paths.

The influence of small perturbations of the shape onto an existing set of paths may thus be modeled by node and edge insertions along these paths. In order to get a path kernel robust against structural noise we associate to each path a sequence of successively reduced paths, thus forming a hierarchy of paths. Our implicit assumption is that, if a path has been elongated by structural noise one of its reduced version should corresponds to the original path.

The reduction of a path is performed either by node removal or edge contraction along the path. Such a set of reduction operations is compatible with the taxinomy of topological transition of the skeleton compiled by Giblin and Kimia [12]. Note that, since all vertices have a degree lower than 2 along the path these operations are well defined. In order to select both the type of operation and the node or the edge to respectively remove or contract we have to associate a weight to each node and edge which reflects its importance according to the considered path and the whole graph.

Let us consider a skeletal graph G, its associated maximal spanning tree T and a path $h = (v_1, \ldots, v_n)$ within T. We valuate each operation on h as follows:

Node removal : Let us denote by v_i, $i \in \{2, \ldots, n-1\}$ the removed node of the path h. The node v_i has a degree greater than 2 in T by construction. Our basic idea consists to valuate the importance of v_i by the total weight of the additional branches which justify its existence within the path h. For

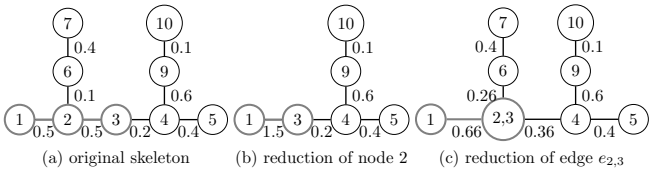

Fig. 2. Different reductions of a path (in gray) within a skeletal tree.

each neighbor v of v_i not equal to v_{i-1} nor v_{i+1} we compute the weight $W(v)$ defined as the addition of the weight of the tree rooted on v in $T - \{e_{v_i v}\}$ and the weight of $e_{v_i v}$. This tree is unique since T is a tree. The weight of the node v_i (and the cost of its removal) is then defined as the sum of weight $W(v)$ for all neighbors v of v_i (excluding v_{i-1} and v_i).
After the removal of this node the edges $e_{v_{i-1}v_i}$ and $e_{v_i v_{i+1}}$ are concatenated into a single edge in the new path h'. The weight of this new edge is defined as the sum of the weight of the edges $e_{v_{i-1}v_i}$, $e_{v_i v_{i+1}}$ and the weight of the node v_i (Fig. 2(a) and (b)).

Edge contraction : The cost of an edge contraction is measured by the relevance of the edge which is encoded by its weight. Let us denote by $e_{v_i v_{i+1}}$, $i < n$ the contracted edge of the path $h = (v_1, \ldots, v_n)$. In order to preserve the total weight of the tree after the contraction, the weight of the edge $e_{v_i v_{i+1}}$ is equally distributed among the edges of T incident to v_i and v_{i+1}:

$$\forall e \in \iota(v_i) \cup \iota(v_{i+1}) - \{e_{v_i v_{i+1}}\} \quad w'(e) = w(e) + \frac{w(e_{v_i v_{i+1}})}{d(v_i) + d(v_{i+1}) - 2}$$

where $\iota(v)$ and $d(v)$ denote respectively the set of edges incident to v and the cardinal of this set (the vertex's degree). The symbol $w(e)$ denotes the weight of the edge e.
For example, the contraction of the edge $e_{2,3}$ in Fig. 2(a) corresponds to a cost of $w(e_{2,3}) = .5$. The contraction of this edge induces the incrementation of the edge's weights $w(e_{2,1})$,$w(e_{2,6})$,$w(e_{3,4})$ by $.5/3 \approx .16$

Any additive measure encoding the relevance of a branch of the skeleton may be used as a weight. We choose to use the measure defined by Torsello [13] which associates to each branch of the skeleton (an thus to each edge) the length of the boundaries which contributed to the creation of this branch. Such a measure initially defined for each pixel of the skeleton is trivially additive.

Let us denote by κ the function which applies the cheapest operation on a path. The successive applications of the function κ associate to each path h a sequence of reduced paths $(h, \kappa(h), \ldots, \kappa^D(h))$ where D denotes the maximal number of reductions. Using $K_{classic}$ for the path comparison, we define the kernel K_{edit} as the mean value of kernels between reduced paths of equal length. Given two paths h and h', this kernel is thus equal to 0 if $||h| - |h'|| > D$. Indeed, in this case the maximal reduction of the longuest path remains longuer than

the shortest one. Otherwise, $||h| - |h'|| \leq D$, and $K_{edit}(h, h')$ is defined as:

$$K_{edit}(h, h') = \frac{1}{D+1} \sum_{k=0}^{D} \sum_{l=0}^{D} K_{classic}(\kappa^k(h), \kappa^l(h')) \tag{7}$$

This kernel is proportional (by a factor $D + 1$) to a sum of R-convolution kernels [14, Lemma 1] and is thus definite positive.

Since $K_{classic}$ is equal to 0 for paths of different lengths, K_{edit} is indeed equal to a sum of kernels between reduced paths of equal length. For example, given two paths h and h' whose respective length is equal to 4 and 3 we have for $D = 2$:

$$K_{edit}(h, h') = \frac{1}{3} \left[K_{classic}(\kappa(h), h') + K_{classic}(\kappa^2(h), \kappa(h')) \right]$$

4 Experiments

We used the following features for our experiments: Each node is weighted by its distance to the gravity center of the shape and each edge is assocated to a vector of two features: The first feature corresponds to the edge's weight (section 3.2). The second feature is the angle between the straight line passing through the two nodes of the edge and the principal axis of the shape. These experiments are based on the LEMS [15] database which consists of 99 objects divided into 9 classes.

We defined three kernels for these experiments: The kernel $K_{max,classic}$ based on a conjoint use of the kernels K_{max} (equation 2) and $K_{classic}$ (equation 4) has been introduced by Suard [6]. The kernel $K_{change,classic}$ based on a conjoint use of the kernels K_{change} (equation 6) and $K_{classic}$ allows to evaluate the performances of the kernel K_{change} compared to the kernel K_{max}. Finally, the kernel K_{new} is based on a conjoint used of the two kernels K_{edit} and K_{change} proposed in this paper. The kernel $K_{classic}$ is defined by the two parameters σ_{edge} and σ_{vertex} respectively used by the Gaussian RBF kernels on edges and vertices. The kernel $K_{max,classic}$ does not require additional parameters while $K_{change,classic}$ is based on a ν-SVM and requires thus the parameter ν. It additionally requires the parameter $\sigma_{change}^{classic}$ used by the RBF kernel in equation 6. The kernel K_{edit} requires the two parameters σ_{edge} and σ_{vertex} used by $K_{classic}$ together with the maximal number of edition (D). Finally, the kernel K_{new} requires as K_{change} the two additional parameters ν and σ_{change}^{new}(equation 6). These parameters have been fixed to the following values in the experiments described below: $D = 2$, $\sigma_{edge} = \sigma_{vertex} = 0.1$, $\nu = 0.9$, $\sigma_{change}^{new} = 0.3$ and $\sigma_{change}^{classic} = 1.0$. The parameters σ_{edge} and σ_{vertex} are common to all kernels. The remaining parameters have been been set in order to maximize the performances of each kernel on the experiments below.

Our first experiment compares the distance induced by each kernel k and defined as $d^2(x, x') = k(x, x) + k(x', x') - 2k(x, x')$. The mean number of matches for each class is defined as follows: For each shape of the selected class we sort all the shapes of the database according to their distances to the selected shape

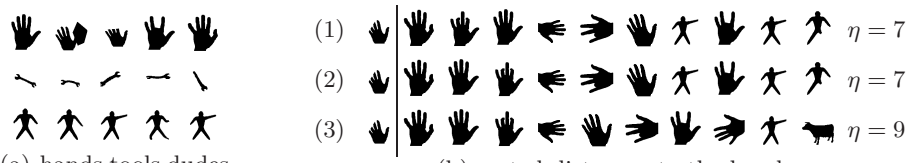

(a) hands,tools,dudes (b) sorted distances to the hand

Fig. 3. Five representative shapes of the classes hands, tools and dudes of the LEMS database (a), and (b) the 10 closest shapes from an hand using the distances induced by the kernels $K_{max,classic}$ (1), $K_{change,classic}$ (2) and K_{new} (3).

using an ascending order. The number of good matches of the input shape is then defined as the number of shapes ranked before the first shape which belongs to a different class than the selected one. For example, the 10 nearest neighbors of a hand sorted in an ascending order are represented in Fig. 3(b), the number of good matches of each shape is indicated on the right of the figure. Note that the greater number of good match being obtained for the kernel K_{new}. The mean number of good matches of a class is defined as the mean value of the number of good matches for each shape of the class. The different values represented in Tab. 1(a) represent the mean values of these number of good matches for the classes: hands, tools and dudes (Fig. 3(a)). As indicated by Tab. 1(a), the kernel $K_{max,classic}$ provides stable results but is sensitive to slight perturbations of the shapes as the ones of the class dudes and cannot handle the severe modifications of the hands. The kernel $K_{change,classic}$ leads to roughly similar results on the different classes. Though not presented here, the kernel $K_{matching,classic}$ (equation 3) gives worst results than the others kernels. This result may be explained by the drawbacks of this kernel (Section 2.2). The kernel K_{new} always provides the best results with a good robustness to perturbation on dudes and hands.

Our second experiment evaluates performances of each kernel within a classification framework. To this end, we have trained a SVM on 5 shapes of each of the three classes: dudes, hands, tools on one side and one model of each of the 6 remaining classes on the other side. The SVM margin parameter was selected in order to maximize the number of true positive while having no false positive. Tab. 1(b) shows the number of well classified shapes for each class. The kernel

	Hands	Tools	Dudes
$K_{max,classic}$	4.81	6.18	6.36
$K_{change,classic}$	5.27	5.45	6.36
K_{new}	7.09	9.82	6.36

(a) Mean number of good matches.

	Hands	Tools	Dudes
$K_{max,classic}$	7	11	10
$K_{change,classic}$	7	10	10
K_{new}	9	11	11

(b) Number of recognized shapes in one class.

Table 1. Kernels evaluation based on distance (a) and classification (b) criteria.

K_{new} gives the best performances especially for the hands where the two missing shapes are the more perturbed ones. The two others kernels present good results and are competitive when shapes are not strongly deformed. This experiment confirms the robustness of our kernel against perturbed shapes.

5 Conclusion

The bag of path approach is based on a decomposition of the complex graph structure into a set of linear objects (paths). Such an approach benefits of recent advances in both string and vectors kernels. Our graph kernel based on a hierarchy of paths is more stable to small perturbations of the shapes than kernels based solely on a bag of paths. Our notion of path's hierarchy is related to the graph edit distance through the successive rewritings of a path. Our kernel is thus related to the ones introduced by Neuhaus and Bunke.

References

1. Sharvit, D., Chan, J., Tek, H., Kimia, B.: Symmetry-based indexing of image databases. Journal of Visual Communication and Image Representation **9**(4) (Dec. 1998) 366–380
2. Siddiqi, K., Shokoufandeh, A., Dickinson, S.J., Zucker, S.W.: Shock graphs and shape matching. Int. J. Comput. Vision **35**(1) (1999) 13–32
3. Pelillo, M., Siddiqi, K., Zucker, S.: Matching hierarchical structures using association graphs. IEEE Trans. on PAMI **21**(11) (Nov 1999) 1105–1120
4. Bunke, H., Riesen, K.: A family of novel graph kernels for structural pattern recognition. In: CIARP. (2007) 20–31
5. Neuhaus, M., Bunke, H.: Edit distance based kernel functions for structural pattern classification. Pattern Recognition **39** (2006) 1852–1863
6. Suard, F., Rakotomamonjy, A., Bensrhair, A.: Kernel on bag of paths for measuring similarity of shapes. In: European Symposium on Artificial Neural Networks, Bruges-Belgique (April 2007)
7. Haasdonk, B.: Feature space interpretation of svms with indefinite kernels. IEEE PAMI **27**(4) (April 2005) 482–492
8. Desobry, F., Davy, M., Doncarli, C.: An online kernel change detection algorithm. IEEE TSP **53**(8) (August 2005) 2961–2974
9. Kashima, H., Tsuda, K., Inokuchi, A.: Marginalized kernel between labeled graphs. In: In Proc. of the Twentieth International conference on machine Learning. (2003)
10. Ruberto, C.D.: Recognition of shapes by attributed skeletal graphs. Pattern Recognition **37**(1) (2004) 21–31
11. Berg, C., Christensen, J.P.R., Ressel, P.: Harmonic Analysis on Semigroups. Springer-Verlag (1984)
12. Giblin, P.J., Kimia, B.B.: On the local form and transitions of symmetry sets, medial axes, and shocks. In: Seventh Internat. Conf. on Computer Vision. (1999) 385–391
13. Torsello, A., Handcock, E.R.: A skeletal measure of 2d shape similarity. CVIU **95** (2004) 1–29
14. Haussler, D.: Convolution kernels on discrete structures. Technical report, Department of Computer Science, University of California at Santa Cruz (1999)
15. LEMS: shapes databases. http://www.lems.brown.edu/vision/software/index.html

arXiv:0810.3579v1 [cs.CV] 20 Oct 2008

Preface

This textbook is intended for use by students of physics, physical chemistry, and theoretical chemistry. The reader is presumed to have a basic knowledge of atomic and quantum physics at the level provided, for example, by the first few chapters in our book *The Physics of Atoms and Quanta*. The student of physics will find here material which should be included in the basic education of every physicist. This book should furthermore allow students to acquire an appreciation of the breadth and variety within the field of molecular physics and its future as a fascinating area of research.

For the student of chemistry, the concepts introduced in this book will provide a theoretical framework for that entire field of study. With the help of these concepts, it is at least in principle possible to reduce the enormous body of empirical chemical knowledge to a few basic principles: those of quantum mechanics. In addition, modern physical methods whose fundamentals are introduced here are becoming increasingly important in chemistry and now represent indispensable tools for the chemist. As examples, we might mention the structural analysis of complex organic compounds, spectroscopic investigation of very rapid reaction processes or, as a practical application, the remote detection of pollutants in the air.

April 1995

Walter Olthoff
Program Chair
ECOOP'95

Organization

ECOOP'95 is organized by the department of Computer Science, Univeristy of Århus and AITO (association Internationa pour les Technologie Object) in cooperation with ACM/SIGPLAN.

Executive Commitee

Conference Chair:	Ole Lehrmann Madsen (Århus University, DK)
Program Chair:	Walter Olthoff (DFKI GmbH, Germany)
Organizing Chair:	Jørgen Lindskov Knudsen (Århus University, DK)
Tutorials:	Birger Møller-Pedersen (Norwegian Computing Center, Norway)
Workshops:	Eric Jul (University of Kopenhagen, Denmark)
Panels:	Boris Magnusson (Lund University, Sweden)
Exhibition:	Elmer Sandvad (Århus University, DK)
Demonstrations:	Kurt Nørdmark (Århus University, DK)

Program Commitee

Conference Chair:	Ole Lehrmann Madsen (Århus University, DK)
Program Chair:	Walter Olthoff (DFKI GmbH, Germany)
Organizing Chair:	Jørgen Lindskov Knudsen (Århus University, DK)
Tutorials:	Birger Møller-Pedersen (Norwegian Computing Center, Norway)
Workshops:	Eric Jul (University of Kopenhagen, Denmark)
Panels:	Boris Magnusson (Lund University, Sweden)
Exhibition:	Elmer Sandvad (Århus University, DK)
Demonstrations:	Kurt Nørdmark (Århus University, DK)

Referees

V. Andreev	Braunschweig	P. Dingus
Bärwolff	F.W. Büsser	H. Duhm
E. Barrelet	T. Carli	J. Ebert
H.P. Beck	A.B. Clegg	S. Eichenberger
G. Bernardi	G. Cozzika	R.J. Ellison
E. Binder	S. Dagoret	Feltesse
P.C. Bosetti	Del Buono	W. Flauger

A. Fomenko
G. Franke
J. Garvey
M. Gennis
L. Goerlich
P. Goritchev
H. Greif
E.M. Hanlon
R. Haydar
R.C.W. Henderso
P. Hill
H. Hufnagel
A. Jacholkowska
Johannsen
S. Kasarian
I.R. Kenyon
C. Kleinwort
T. Köhler
S.D. Kolya
P. Kostka
U. Krüger
J. Kurzhöfer
M.P.J. Landon
A. Lebedev
Ch. Ley
F. Linsel
H. Lohmand
Martin
S. Masson
K. Meier
C.A. Meyer
S. Mikocki
J.V. Morris
B. Naroska
Nguyen
U. Obrock
G.D. Patel
Ch. Pichler
S. Prell
F. Raupach
V. Riech
P. Robmann
N. Sahlmann
P. Schleper
Schöning
B. Schwab
A. Semenov
G. Siegmon
J.R. Smith
M. Steenbock
U. Straumann
C. Thiebaux
P. Van Esch
from Yerevan Ph
L.R. West
G.-G. Winter
T.P. Yiou
M. Zimmer

Sponsoring Institutions

Bernauer-Budiman Inc., Reading, Mass.
The Hofmann-International Company, San Louis Obispo, Cal.
Kramer Industries, Heidelberg, Germany

Table of Contents

Hamiltonian Mechanics

Hamiltonian Mechanics unter besonderer Berücksichtigung der höhreren Lehranstalten 1
Ivar Ekeland, Roger Temam, Jeffrey Dean, David Grove, Craig Chambers, Kim B. Bruce, Elisa Bertino

Hamiltonian Mechanics2 7
Ivar Ekeland and Roger Temam

Author Index 13

Subject Index 17

Hamiltonian Mechanics unter besonderer Berücksichtigung der höhreren Lehranstalten

Ivar Ekeland[1], Roger Temam[2] Jeffrey Dean, David Grove, Craig Chambers, Kim B. Bruce, and Elsa Bertino

[1] Princeton University, Princeton NJ 08544, USA,
I.Ekeland@princeton.edu,
WWW home page: http://users/~iekeland/web/welcome.html
[2] Université de Paris-Sud, Laboratoire d'Analyse Numérique, Bâtiment 425, F-91405 Orsay Cedex, France

Abstract. The abstract should summarize the contents of the paper using at least 70 and at most 150 words. It will be set in 9-point font size and be inset 1.0 cm from the right and left margins. There will be two blank lines before and after the Abstract. ...

1 Fixed-Period Problems: The Sublinear Case

With this chapter, the preliminaries are over, and we begin the search for periodic solutions to Hamiltonian systems. All this will be done in the convex case; that is, we shall study the boundary-value problem

$$\begin{aligned} \dot{x} &= JH'(t,x) \\ x(0) &= x(T) \end{aligned}$$

with $H(t,\cdot)$ a convex function of x, going to $+\infty$ when $\|x\| \to \infty$.

1.1 Autonomous Systems

In this section, we will consider the case when the Hamiltonian $H(x)$ is autonomous. For the sake of simplicity, we shall also assume that it is C^1.

We shall first consider the question of nontriviality, within the general framework of (A_∞, B_∞)-subquadratic Hamiltonians. In the second subsection, we shall look into the special case when H is $(0, b_\infty)$-subquadratic, and we shall try to derive additional information.

The General Case: Nontriviality. We assume that H is (A_∞, B_∞)-subquadratic at infinity, for some constant symmetric matrices A_∞ and B_∞, with $B_\infty - A_\infty$ positive definite. Set:

$$\gamma := \text{smallest eigenvalue of } \ B_\infty - A_\infty \tag{1}$$

$$\lambda := \text{largest negative eigenvalue of } \ J\frac{d}{dt} + A_\infty \ . \tag{2}$$

Theorem 1 tells us that if $\lambda + \gamma < 0$, the boundary-value problem:

$$\begin{aligned} \dot{x} &= JH'(x) \\ x(0) &= x(T) \end{aligned} \tag{3}$$

has at least one solution $\overline{x}$, which is found by minimizing the dual action functional:

$$\psi(u) = \int_o^T \left[\frac{1}{2} \left(\Lambda_o^{-1} u, u \right) + N^*(-u) \right] dt \tag{4}$$

on the range of Λ, which is a subspace $R(\Lambda)_L^2$ with finite codimension. Here

$$N(x) := H(x) - \frac{1}{2} \left(A_\infty x, x \right) \tag{5}$$

is a convex function, and

$$N(x) \leq \frac{1}{2} \left(\left(B_\infty - A_\infty \right) x, x \right) + c \quad \forall x \ . \tag{6}$$

Proposition 1. *Assume $H'(0) = 0$ and $H(0) = 0$. Set:*

$$\delta := \liminf_{x \to 0} 2N(x) \left\| x \right\|^{-2} \ . \tag{7}$$

If $\gamma < -\lambda < \delta$, the solution $\overline{u}$ is non-zero:

$$\overline{x}(t) \neq 0 \quad \forall t \ . \tag{8}$$

Proof. Condition (7) means that, for every $\delta' > \delta$, there is some $\varepsilon > 0$ such that

$$\left\| x \right\| \leq \varepsilon \Rightarrow N(x) \leq \frac{\delta'}{2} \left\| x \right\|^2 \ . \tag{9}$$

It is an exercise in convex analysis, into which we shall not go, to show that this implies that there is an $\eta > 0$ such that

$$f \left\| x \right\| \leq \eta \Rightarrow N^*(y) \leq \frac{1}{2\delta'} \left\| y \right\|^2 \ . \tag{10}$$

Fig. 1. This is the caption of the figure displaying a white eagle and a white horse on a snow field

Since u_1 is a smooth function, we will have $\|hu_1\|_\infty \leq \eta$ for h small enough, and inequality (10) will hold, yielding thereby:

$$\psi(hu_1) \leq \frac{h^2}{2}\frac{1}{\lambda}\|u_1\|_2^2 + \frac{h^2}{2}\frac{1}{\delta'}\|u_1\|^2 \ . \tag{11}$$

If we choose δ' close enough to δ, the quantity $\left(\frac{1}{\lambda}+\frac{1}{\delta'}\right)$ will be negative, and we end up with

$$\psi(hu_1) < 0 \qquad \text{for} \quad h \neq 0 \ \text{ small} \ . \tag{12}$$

On the other hand, we check directly that $\psi(0) = 0$. This shows that 0 cannot be a minimizer of ψ, not even a local one. So $\overline{u} \neq 0$ and $\overline{u} \neq \Lambda_o^{-1}(0) = 0$. □

Corollary 1. *Assume H is C^2 and (a_∞, b_∞)-subquadratic at infinity. Let ξ_1, $\ldots, \xi_N$ be the equilibria, that is, the solutions of $H'(\xi) = 0$. Denote by ω_k the smallest eigenvalue of $H''(\xi_k)$, and set:*

$$\omega := \text{Min}\ \{\omega_1, \ldots, \omega_k\} \ . \tag{13}$$

If:

$$\frac{T}{2\pi}b_\infty < -E\left[-\frac{T}{2\pi}a_\infty\right] < \frac{T}{2\pi}\omega \tag{14}$$

then minimization of ψ yields a non-constant T-periodic solution $\overline{x}$.

We recall once more that by the integer part $E[\alpha]$ of $\alpha \in \mathbb{R}$, we mean the $a \in \mathbb{Z}$ such that $a < \alpha \leq a+1$. For instance, if we take $a_\infty = 0$, Corollary 2 tells us that $\overline{x}$ exists and is non-constant provided that:

$$\frac{T}{2\pi}b_\infty < 1 < \frac{T}{2\pi} \tag{15}$$

or

$$T \in \left(\frac{2\pi}{\omega}, \frac{2\pi}{b_\infty}\right) \ . \tag{16}$$

Proof. The spectrum of Λ is $\frac{2\pi}{T}\mathbb{Z} + a_\infty$. The largest negative eigenvalue λ is given by $\frac{2\pi}{T}k_o + a_\infty$, where

$$\frac{2\pi}{T}k_o + a_\infty < 0 \leq \frac{2\pi}{T}(k_o+1) + a_\infty \ . \tag{17}$$

Hence:

$$k_o = E\left[-\frac{T}{2\pi}a_\infty\right] \ . \tag{18}$$

The condition $\gamma < -\lambda < \delta$ now becomes:

$$b_\infty - a_\infty < -\frac{2\pi}{T}k_o - a_\infty < \omega - a_\infty \tag{19}$$

which is precisely condition (14). □

Lemma 1. *Assume that H is C^2 on $\mathbb{R}^{2n}\backslash\{0\}$ and that $H''(x)$ is non-degenerate for any $x \neq 0$. Then any local minimizer $\widetilde{x}$ of ψ has minimal period T.*

Proof. We know that $\widetilde{x}$, or $\widetilde{x} + \xi$ for some constant $\xi \in \mathbb{R}^{2n}$, is a T-periodic solution of the Hamiltonian system:

$$\dot{x} = JH'(x) \ . \tag{20}$$

There is no loss of generality in taking $\xi = 0$. So $\psi(x) \geq \psi(\widetilde{x})$ for all $\widetilde{x}$ in some neighbourhood of x in $W^{1,2}\left(\mathbb{R}/T\mathbb{Z}; \mathbb{R}^{2n}\right)$.

But this index is precisely the index $i_T(\widetilde{x})$ of the T-periodic solution $\widetilde{x}$ over the interval $(0, T)$, as defined in Sect. 2.6. So

$$i_T(\widetilde{x}) = 0 \ . \tag{21}$$

Now if $\widetilde{x}$ has a lower period, T/k say, we would have, by Corollary 31:

$$i_T(\widetilde{x}) = i_{kT/k}(\widetilde{x}) \geq k i_{T/k}(\widetilde{x}) + k - 1 \geq k - 1 \geq 1 \ . \tag{22}$$

This would contradict (21), and thus cannot happen. □

Notes and Comments. The results in this section are a refined version of [1]; the minimality result of Proposition 14 was the first of its kind.

To understand the nontriviality conditions, such as the one in formula (16), one may think of a one-parameter family x_T, $T \in \left(2\pi\omega^{-1}, 2\pi b_\infty^{-1}\right)$ of periodic solutions, $x_T(0) = x_T(T)$, with x_T going away to infinity when $T \to 2\pi\omega^{-1}$, which is the period of the linearized system at 0.

Table 1. This is the example table taken out of *The TEXbook,* p. 246

Year	World population
8000 B.C.	5,000,000
50 A.D.	200,000,000
1650 A.D.	500,000,000
1945 A.D.	2,300,000,000
1980 A.D.	4,400,000,000

Theorem 1 (Ghoussoub-Preiss). *Assume $H(t, x)$ is $(0, \varepsilon)$-subquadratic at infinity for all $\varepsilon > 0$, and T-periodic in t*

$$H(t, \cdot) \qquad \text{is convex} \quad \forall t \tag{23}$$

$$H(\cdot, x) \qquad \text{is} \quad T-\text{periodic} \quad \forall x \tag{24}$$

$$H(t, x) \geq n\left(\|x\|\right) \qquad \text{with} \quad n(s)s^{-1} \to \infty \quad \text{as} \quad s \to \infty \tag{25}$$

$$\forall \varepsilon > 0 \ , \quad \exists c \ : \ H(t,x) \leq \frac{\varepsilon}{2} \left\| x \right\|^2 + c \ . \tag{26}$$

Assume also that H is C^2, and $H''(t,x)$ is positive definite everywhere. Then there is a sequence x_k, $k \in \mathbb{N}$, of kT-periodic solutions of the system

$$\dot{x} = JH'(t,x) \tag{27}$$

such that, for every $k \in \mathbb{N}$, there is some $p_o \in \mathbb{N}$ with:

$$p \geq p_o \Rightarrow x_{pk} \neq x_k \ . \tag{28}$$

□

*Example 1 (*External forcing*).* Consider the system:

$$\dot{x} = JH'(x) + f(t) \tag{29}$$

where the Hamiltonian H is $(0, b_\infty)$-subquadratic, and the forcing term is a distribution on the circle:

$$f = \frac{d}{dt} F + f_o \qquad \text{with} \ \ F \in L^2 \left(\mathbb{R}/T\mathbb{Z}; \mathbb{R}^{2n} \right) \ , \tag{30}$$

where $f_o := T^{-1} \int_o^T f(t) dt$. For instance,

$$f(t) = \sum_{k \in \mathbb{N}} \delta_k \xi \ , \tag{31}$$

where δ_k is the Dirac mass at $t = k$ and $\xi \in \mathbb{R}^{2n}$ is a constant, fits the prescription. This means that the system $\dot{x} = JH'(x)$ is being excited by a series of identical shocks at interval T.

Definition 1. *Let $A_\infty(t)$ and $B_\infty(t)$ be symmetric operators in $\mathbb{R}^{2n}$, depending continuously on $t \in [0,T]$, such that $A_\infty(t) \leq B_\infty(t)$ for all t.*

A Borelian function $H : [0,T] \times \mathbb{R}^{2n} \to \mathbb{R}$ is called (A_∞, B_∞)-subquadratic at infinity if there exists a function $N(t,x)$ such that:

$$H(t,x) = \frac{1}{2} \left(A_\infty(t) x, x \right) + N(t,x) \tag{32}$$

$$\forall t \ , \quad N(t,x) \qquad \text{is convex with respect to} \ \ x \tag{33}$$

$$N(t,x) \geq n\left(\left\| x \right\| \right) \qquad \text{with} \ \ n(s) s^{-1} \to +\infty \ \ \text{as} \ \ s \to +\infty \tag{34}$$

$$\exists c \in \mathbb{R} \ : \quad H(t,x) \leq \frac{1}{2} \left(B_\infty(t) x, x \right) + c \quad \forall x \ . \tag{35}$$

If $A_\infty(t) = a_\infty I$ and $B_\infty(t) = b_\infty I$, with $a_\infty \leq b_\infty \in \mathbb{R}$, we shall say that H is (a_∞, b_∞)-subquadratic at infinity. As an example, the function $\left\| x \right\|^\alpha$, with $1 \leq \alpha < 2$, is $(0, \varepsilon)$-subquadratic at infinity for every $\varepsilon > 0$. Similarly, the Hamiltonian

$$H(t,x) = \frac{1}{2} k \left\| k \right\|^2 + \left\| x \right\|^\alpha \tag{36}$$

is $(k, k+\varepsilon)$-subquadratic for every $\varepsilon > 0$. Note that, if $k < 0$, it is not convex.

Notes and Comments. The first results on subharmonics were obtained by Rabinowitz in [5], who showed the existence of infinitely many subharmonics both in the subquadratic and superquadratic case, with suitable growth conditions on H'. Again the duality approach enabled Clarke and Ekeland in [2] to treat the same problem in the convex-subquadratic case, with growth conditions on H only.

Recently, Michalek and Tarantello (see [3] and [4]) have obtained lower bound on the number of subharmonics of period kT, based on symmetry considerations and on pinching estimates, as in Sect. 5.2 of this article.

References

1. Clarke, F., Ekeland, I.: Nonlinear oscillations and boundary-value problems for Hamiltonian systems. Arch. Rat. Mech. Anal. 78, 315–333 (1982)
2. Clarke, F., Ekeland, I.: Solutions périodiques, du période donnée, des équations hamiltoniennes. Note CRAS Paris 287, 1013–1015 (1978)
3. Michalek, R., Tarantello, G.: Subharmonic solutions with prescribed minimal period for nonautonomous Hamiltonian systems. J. Diff. Eq. 72, 28–55 (1988)
4. Tarantello, G.: Subharmonic solutions for Hamiltonian systems via a $\mathbb{Z}_p$ pseudoindex theory. Annali di Matematica Pura (to appear)
5. Rabinowitz, P.: On subharmonic solutions of a Hamiltonian system. Comm. Pure Appl. Math. 33, 609–633 (1980)

Hamiltonian Mechanics2

Ivar Ekeland[1] and Roger Temam[2]

[1] Princeton University, Princeton NJ 08544, USA
[2] Université de Paris-Sud, Laboratoire d'Analyse Numérique, Bâtiment 425, F-91405 Orsay Cedex, France

Abstract. The abstract should summarize the contents of the paper using at least 70 and at most 150 words. It will be set in 9-point font size and be inset 1.0 cm from the right and left margins. There will be two blank lines before and after the Abstract. ...

1 Fixed-Period Problems: The Sublinear Case

With this chapter, the preliminaries are over, and we begin the search for periodic solutions to Hamiltonian systems. All this will be done in the convex case; that is, we shall study the boundary-value problem

$$\begin{aligned} \dot{x} &= JH'(t,x) \\ x(0) &= x(T) \end{aligned}$$

with $H(t,\cdot)$ a convex function of x, going to $+\infty$ when $\|x\| \to \infty$.

1.1 Autonomous Systems

In this section, we will consider the case when the Hamiltonian $H(x)$ is autonomous. For the sake of simplicity, we shall also assume that it is C^1.

We shall first consider the question of nontriviality, within the general framework of (A_∞, B_∞)-subquadratic Hamiltonians. In the second subsection, we shall look into the special case when H is $(0, b_\infty)$-subquadratic, and we shall try to derive additional information.

The General Case: Nontriviality. We assume that H is (A_∞, B_∞)-subquadratic at infinity, for some constant symmetric matrices A_∞ and B_∞, with $B_\infty - A_\infty$ positive definite. Set:

$$\gamma := \text{smallest eigenvalue of } \ B_\infty - A_\infty \tag{1}$$

$$\lambda := \text{largest negative eigenvalue of } \ J\frac{d}{dt} + A_\infty \ . \tag{2}$$

Theorem 21 tells us that if $\lambda + \gamma < 0$, the boundary-value problem:

$$\begin{aligned} \dot{x} &= JH'(x) \\ x(0) &= x(T) \end{aligned} \tag{3}$$

has at least one solution $\overline{x}$, which is found by minimizing the dual action functional:

$$\psi(u) = \int_o^T \left[\frac{1}{2} \left(\Lambda_o^{-1} u, u \right) + N^*(-u) \right] dt \tag{4}$$

on the range of Λ, which is a subspace $R(\Lambda)_L^2$ with finite codimension. Here

$$N(x) := H(x) - \frac{1}{2} \left(A_\infty x, x \right) \tag{5}$$

is a convex function, and

$$N(x) \leq \frac{1}{2} \left(\left(B_\infty - A_\infty \right) x, x \right) + c \quad \forall x \ . \tag{6}$$

Proposition 1. *Assume $H'(0) = 0$ and $H(0) = 0$. Set:*

$$\delta := \liminf_{x \to 0} 2N(x) \left\| x \right\|^{-2} \ . \tag{7}$$

If $\gamma < -\lambda < \delta$, the solution $\overline{u}$ is non-zero:

$$\overline{x}(t) \neq 0 \quad \forall t \ . \tag{8}$$

Proof. Condition (7) means that, for every $\delta' > \delta$, there is some $\varepsilon > 0$ such that

$$\left\| x \right\| \leq \varepsilon \Rightarrow N(x) \leq \frac{\delta'}{2} \left\| x \right\|^2 \ . \tag{9}$$

It is an exercise in convex analysis, into which we shall not go, to show that this implies that there is an $\eta > 0$ such that

$$f \left\| x \right\| \leq \eta \Rightarrow N^*(y) \leq \frac{1}{2\delta'} \left\| y \right\|^2 \ . \tag{10}$$

Fig. 1. This is the caption of the figure displaying a white eagle and a white horse on a snow field

Since u_1 is a smooth function, we will have $\left\| h u_1 \right\|_\infty \leq \eta$ for h small enough, and inequality (10) will hold, yielding thereby:

$$\psi(h u_1) \leq \frac{h^2}{2} \frac{1}{\lambda} \left\| u_1 \right\|_2^2 + \frac{h^2}{2} \frac{1}{\delta'} \left\| u_1 \right\|^2 \ . \tag{11}$$

If we choose δ' close enough to δ, the quantity $\left(\frac{1}{\lambda}+\frac{1}{\delta'}\right)$ will be negative, and we end up with

$$\psi(hu_1)<0 \qquad \text{for} \quad h\neq 0 \quad \text{small} \ . \tag{12}$$

On the other hand, we check directly that $\psi(0)=0$. This shows that 0 cannot be a minimizer of ψ, not even a local one. So $\overline{u}\neq 0$ and $\overline{u}\neq \Lambda_o^{-1}(0)=0$. □

Corollary 1. *Assume H is C^2 and (a_∞,b_∞)-subquadratic at infinity. Let ξ_1, $\dots,\xi_N$ be the equilibria, that is, the solutions of $H'(\xi)=0$. Denote by ω_k the smallest eigenvalue of $H''(\xi_k)$, and set:*

$$\omega := \text{Min}\ \{\omega_1,\dots,\omega_k\} \ . \tag{13}$$

If:

$$\frac{T}{2\pi}b_\infty < -E\left[-\frac{T}{2\pi}a_\infty\right] < \frac{T}{2\pi}\omega \tag{14}$$

then minimization of ψ yields a non-constant T-periodic solution $\overline{x}$.

We recall once more that by the integer part $E[\alpha]$ of $\alpha\in\mathbb{R}$, we mean the $a\in\mathbb{Z}$ such that $a<\alpha\leq a+1$. For instance, if we take $a_\infty=0$, Corollary 2 tells us that $\overline{x}$ exists and is non-constant provided that:

$$\frac{T}{2\pi}b_\infty<1<\frac{T}{2\pi} \tag{15}$$

or

$$T\in\left(\frac{2\pi}{\omega},\frac{2\pi}{b_\infty}\right) \ . \tag{16}$$

Proof. The spectrum of Λ is $\frac{2\pi}{T}\mathbb{Z}+a_\infty$. The largest negative eigenvalue λ is given by $\frac{2\pi}{T}k_o+a_\infty$, where

$$\frac{2\pi}{T}k_o+a_\infty<0\leq\frac{2\pi}{T}(k_o+1)+a_\infty \ . \tag{17}$$

Hence:

$$k_o=E\left[-\frac{T}{2\pi}a_\infty\right] \ . \tag{18}$$

The condition $\gamma<-\lambda<\delta$ now becomes:

$$b_\infty-a_\infty<-\frac{2\pi}{T}k_o-a_\infty<\omega-a_\infty \tag{19}$$

which is precisely condition (14). □

Lemma 1. *Assume that H is C^2 on $\mathbb{R}^{2n}\backslash\{0\}$ and that $H''(x)$ is non-degenerate for any $x\neq 0$. Then any local minimizer $\widetilde{x}$ of ψ has minimal period T.*

Proof. We know that $\widetilde{x}$, or $\widetilde{x}+\xi$ for some constant $\xi \in \mathbb{R}^{2n}$, is a T-periodic solution of the Hamiltonian system:

$$\dot{x} = JH'(x) \ . \tag{20}$$

There is no loss of generality in taking $\xi = 0$. So $\psi(x) \geq \psi(\widetilde{x})$ for all $\widetilde{x}$ in some neighbourhood of x in $W^{1,2}\left(\mathbb{R}/T\mathbb{Z};\mathbb{R}^{2n}\right)$.

But this index is precisely the index $i_T(\widetilde{x})$ of the T-periodic solution $\widetilde{x}$ over the interval $(0,T)$, as defined in Sect. 2.6. So

$$i_T(\widetilde{x}) = 0 \ . \tag{21}$$

Now if $\widetilde{x}$ has a lower period, T/k say, we would have, by Corollary 31:

$$i_T(\widetilde{x}) = i_{kT/k}(\widetilde{x}) \geq k i_{T/k}(\widetilde{x}) + k - 1 \geq k - 1 \geq 1 \ . \tag{22}$$

This would contradict (21), and thus cannot happen. □

Notes and Comments. The results in this section are a refined version of 1980; the minimality result of Proposition 14 was the first of its kind.

To understand the nontriviality conditions, such as the one in formula (16), one may think of a one-parameter family x_T, $T \in \left(2\pi\omega^{-1}, 2\pi b_\infty^{-1}\right)$ of periodic solutions, $x_T(0) = x_T(T)$, with x_T going away to infinity when $T \to 2\pi\omega^{-1}$, which is the period of the linearized system at 0.

Table 1. This is the example table taken out of *The TEXbook,* p. 246

Year	World population
8000 B.C.	5,000,000
50 A.D.	200,000,000
1650 A.D.	500,000,000
1945 A.D.	2,300,000,000
1980 A.D.	4,400,000,000

Theorem 1 (Ghoussoub-Preiss). *Assume $H(t,x)$ is $(0,\varepsilon)$-subquadratic at infinity for all $\varepsilon > 0$, and T-periodic in t*

$$H(t,\cdot) \qquad \text{is convex} \quad \forall t \tag{23}$$

$$H(\cdot,x) \qquad \text{is} \quad T-\text{periodic} \quad \forall x \tag{24}$$

$$H(t,x) \geq n\left(\|x\|\right) \qquad \text{with} \quad n(s)s^{-1} \to \infty \quad \text{as} \quad s \to \infty \tag{25}$$

$$\forall \varepsilon > 0 \ , \quad \exists c \ : \ H(t,x) \leq \frac{\varepsilon}{2}\|x\|^2 + c \ . \tag{26}$$

Assume also that H is C^2, and $H''(t,x)$ is positive definite everywhere. Then there is a sequence x_k, $k \in \mathbb{N}$, of kT-periodic solutions of the system

$$\dot{x} = JH'(t,x) \tag{27}$$

such that, for every $k \in \mathbb{N}$, there is some $p_o \in \mathbb{N}$ with:

$$p \geq p_o \Rightarrow x_{pk} \neq x_k \ . \tag{28}$$

□

*Example 1 (*External forcing*).* Consider the system:

$$\dot{x} = JH'(x) + f(t) \tag{29}$$

where the Hamiltonian H is $(0, b_\infty)$-subquadratic, and the forcing term is a distribution on the circle:

$$f = \frac{d}{dt}F + f_o \qquad \text{with} \quad F \in L^2\left(\mathbb{R}/T\mathbb{Z}; \mathbb{R}^{2n}\right) \ , \tag{30}$$

where $f_o := T^{-1}\int_o^T f(t)dt$. For instance,

$$f(t) = \sum_{k \in \mathbb{N}} \delta_k \xi \ , \tag{31}$$

where δ_k is the Dirac mass at $t = k$ and $\xi \in \mathbb{R}^{2n}$ is a constant, fits the prescription. This means that the system $\dot{x} = JH'(x)$ is being excited by a series of identical shocks at interval T.

Definition 1. *Let $A_\infty(t)$ and $B_\infty(t)$ be symmetric operators in $\mathbb{R}^{2n}$, depending continuously on $t \in [0,T]$, such that $A_\infty(t) \leq B_\infty(t)$ for all t.*

A Borelian function $H : [0,T] \times \mathbb{R}^{2n} \to \mathbb{R}$ is called (A_∞, B_∞)-subquadratic at infinity if there exists a function $N(t,x)$ such that:

$$H(t,x) = \frac{1}{2}\left(A_\infty(t)x, x\right) + N(t,x) \tag{32}$$

$$\forall t \ , \quad N(t,x) \qquad \text{is convex with respect to} \quad x \tag{33}$$

$$N(t,x) \geq n\left(\|x\|\right) \qquad \text{with} \quad n(s)s^{-1} \to +\infty \quad \text{as} \quad s \to +\infty \tag{34}$$

$$\exists c \in \mathbb{R} \ : \quad H(t,x) \leq \frac{1}{2}\left(B_\infty(t)x, x\right) + c \quad \forall x \ . \tag{35}$$

If $A_\infty(t) = a_\infty I$ and $B_\infty(t) = b_\infty I$, with $a_\infty \leq b_\infty \in \mathbb{R}$, we shall say that H is (a_∞, b_∞)-subquadratic at infinity. As an example, the function $\|x\|^\alpha$, with $1 \leq \alpha < 2$, is $(0, \varepsilon)$-subquadratic at infinity for every $\varepsilon > 0$. Similarly, the Hamiltonian

$$H(t,x) = \frac{1}{2}k\|k\|^2 + \|x\|^\alpha \tag{36}$$

is $(k, k+\varepsilon)$-subquadratic for every $\varepsilon > 0$. Note that, if $k < 0$, it is not convex.

Notes and Comments. The first results on subharmonics were obtained by Rabinowitz in 1985, who showed the existence of infinitely many subharmonics both in the subquadratic and superquadratic case, with suitable growth conditions on H'. Again the duality approach enabled Clarke and Ekeland in 1981 to treat the same problem in the convex-subquadratic case, with growth conditions on H only.

Recently, Michalek and Tarantello (see Michalek, R., Tarantello, G. 1982 and Tarantello, G. 1983) have obtained lower bound on the number of subharmonics of period kT, based on symmetry considerations and on pinching estimates, as in Sect. 5.2 of this article.

References

Clarke, F., Ekeland, I.: Nonlinear oscillations and boundary-value problems for Hamiltonian systems. Arch. Rat. Mech. Anal. 78, 315–333 (1982)

Clarke, F., Ekeland, I.: Solutions périodiques, du période donnée, des équations hamiltoniennes. Note CRAS Paris 287, 1013–1015 (1978)

Michalek, R., Tarantello, G.: Subharmonic solutions with prescribed minimal period for nonautonomous Hamiltonian systems. J. Diff. Eq. 72, 28–55 (1988)

Tarantello, G.: Subharmonic solutions for Hamiltonian systems via a $\mathbb{Z}_p$ pseudoindex theory. Annali di Matematica Pura (to appear)

Rabinowitz, P.: On subharmonic solutions of a Hamiltonian system. Comm. Pure Appl. Math. 33, 609–633 (1980)

Author Index

Abt I. 7
Ahmed T. 3
Andreev V. 24
Andrieu B. 27
Arpagaus M. 34

Babaev A. 25
Bärwolff A. 33
Bán J. 17
Baranov P. 24
Barrelet E. 28
Bartel W. 11
Bassler U. 28
Beck H.P. 35
Behrend H.-J. 11
Berger Ch. 1
Bergstein H. 1
Bernardi G. 28
Bernet R. 34
Besançon M. 9
Biddulph P. 22
Binder E. 11
Bischoff A. 33
Blobel V. 13
Borras K. 8
Bosetti P.C. 2
Boudry V. 27
Brasse F. 11
Braun U. 2
Braunschweig A. 1
Brisson V. 26
Büngener L. 13
Bürger J. 11
Büsser F.W. 13
Buniatian A. 11,37
Buschhorn G. 25

Campbell A.J. 1
Carli T. 25
Charles F. 28
Clarke D. 5
Clegg A.B. 18
Colombo M. 8
Courau A. 26
Coutures Ch. 9
Cozzika G. 9
Criegee L. 11
Cvach J. 27

Dagoret S. 28
Dainton J.B. 19
Dann A.W.E. 22
Dau W.D. 16
Deffur E. 11
Delcourt B. 26
Buono Del A. 28
Devel M. 26
De Roeck A. 11
Dingus P. 27
Dollfus C. 35
Dreis H.B. 2
Drescher A. 8
Düllmann D. 13
Dünger O. 13
Duhm H. 12

Ebbinghaus R. 8
Eberle M. 12
Ebert J. 32
Ebert T.R. 19
Efremenko V. 23
Egli S. 35
Eichenberger S. 35
Eichler R. 34
Eisenhandler E. 20
Ellis N.N. 3
Ellison R.J. 22
Elsen E. 11
Evrard E. 4

Favart L. 4
Feeken D. 13
Felst R. 11
Feltesse A. 9
Fensome I.F. 3
Ferrarotto F. 31
Flamm K. 11
Flauger W. 11
Flieser M. 25
Flügge G. 2

Fomenko A. 24
Fominykh B. 23
Formánek J. 30
Foster J.M. 22
Franke G. 11
Fretwurst E. 12

Gabathuler E. 19
Gamerdinger K. 25
Garvey J. 3
Gayler J. 11
Gellrich A. 13
Gennis M. 11
Genzel H. 1
Godfrey L. 7
Goerlach U. 11
Goerlich L. 6
Gogitidze N. 24
Goodall A.M. 19
Gorelov I. 23
Goritchev P. 23
Grab C. 34
Grässler R. 2
Greenshaw T. 19
Greif H. 25
Grindhammer G. 25

Haack J. 33
Haidt D. 11
Hamon O. 28
Handschuh D. 11
Hanlon E.M. 18
Hapke M. 11
Harjes J. 11
Haydar R. 26
Haynes W.J. 5
Hedberg V. 21
Heinzelmann G. 13
Henderson R.C.W. 18
Henschel H. 33
Herynek I. 29
Hildesheim W. 11
Hill P. 11
Hilton C.D. 22
Hoeger K.C. 22
Huet Ph. 4
Hufnagel H. 14
Huot N. 28

Itterbeck H. 1

Jabiol M.-A. 9
Jacholkowska A. 26
Jacobsson C. 21
Jansen T. 11
Jönsson L. 21
Johannsen A. 13
Johnson D.P. 4
Jung H. 2

Kalmus P.I.P. 20
Kasarian S. 11
Kaschowitz R. 2
Kathage U. 16
Kaufmann H. 33
Kenyon I.R. 3
Kermiche S. 26
Kiesling C. 25
Klein M. 33
Kleinwort C. 13
Knies G. 11
Ko W. 7
Köhler T. 1
Kolanoski H. 8
Kole F. 7
Kolya S.D. 22
Korbel V. 11
Korn M. 8
Kostka P. 33
Kotelnikov S.K. 24
Krehbiel H. 11
Krücker D. 2
Krüger U. 11
Kubenka J.P. 25
Kuhlen M. 25
Kurča T. 17
Kurzhöfer J. 8
Kuznik B. 32

Lamarche F. 27
Lander R. 7
Landon M.P.J. 20
Lange W. 33
Lanius P. 25
Laporte J.F. 9
Lebedev A. 24
Leuschner A. 11
Levonian S. 11,24
Lewin D. 11
Ley Ch. 2
Lindner A. 8

Lindström G. 12
Linsel F. 11
Lipinski J. 13
Loch P. 11
Lohmander H. 21
Lopez G.C. 20

Magnussen N. 32
Mani S. 7
Marage P. 4
Marshall R. 22
Martens J. 32
Martin A.@ 19
Martyn H.-U. 1
Martyniak J. 6
Masson S. 2
Mavroidis A. 20
McMahon S.J. 19
Mehta A. 22
Meier K. 15
Mercer D. 22
Merz T. 11
Meyer C.A. 35
Meyer H. 32
Meyer J. 11
Mikocki S. 6,26
Milone V. 31
Moreau F. 27
Moreels J. 4
Morris J.V. 5
Müller K. 35
Murray S.A. 22

Nagovizin V. 23
Naroska B. 13
Naumann Th. 33
Newton D. 18
Neyret D. 28
Nguyen A. 28
Niebergall F. 13
Nisius R. 1
Nowak G. 6
Nyberg M. 21

Oberlack H. 25
Obrock U. 8
Olsson J.E. 11
Ould-Saada F. 13

Pascaud C. 26
Patel G.D. 19
Peppel E. 11
Phillips H.T. 3
Phillips J.P. 22
Pichler Ch. 12
Pilgram W. 2
Pitzl D. 34
Prell S. 11
Prosi R. 11

Rädel G. 11
Raupach F. 1
Rauschnabel K. 8
Reinshagen S. 11
Ribarics P. 25
Riech V. 12
Riedlberger J. 34
Rietz M. 2
Robertson S.M. 3
Robmann P. 35
Roosen R. 4
Royon C. 9
Rudowicz M. 25
Rusakov S. 24
Rybicki K. 6

Sahlmann N. 2
Sanchez E. 25
Savitsky M. 11
Schacht P. 25
Schleper P. 14
von Schlippe W. 20
Schmidt D. 32
Schmitz W. 2
Schöning A. 11
Schröder V. 11
Schulz M. 11
Schwab B. 14
Schwind A. 33
Seehausen U. 13
Sell R. 11
Semenov A. 23
Shekelyan V. 23
Shooshtari H. 25
Shtarkov L.N. 24
Siegmon G. 16
Siewert U. 16
Skillicorn I.O. 10
Smirnov P. 24
Smith J.R. 7

Smolik L. 11
Spitzer H. 13
Staroba P. 29
Steenbock M. 13
Steffen P. 11
Stella B. 31
Stephens K. 22
Stösslein U. 33
Strachota J. 11
Straumann U. 35
Struczinski W. 2

Taylor R.E. 36,26
Tchernyshov V. 23
Thiebaux C. 27
Thompson G. 20
Truöl P. 35
Turnau J. 6

Urban L. 25
Usik A. 24

Valkarova A. 30
Vallée C. 28
Van Esch P. 4
Vartapetian A. 11
Vazdik Y. 24
Verrecchia P. 9
Vick R. 13
Vogel E. 1

Wacker K. 8
Walther A. 8
Weber G. 13
Wegner A. 11
Wellisch H.P. 25
West L.R. 3
Willard S. 7
Winde M. 33
Winter G.-G. 11
Wolff Th. 34
Wright A.E. 22
Wulff N. 11

Yiou T.P. 28

Žáček J. 30
Zeitnitz C. 12
Ziaeepour H. 26
Zimmer M. 11
Zimmermann W. 11

Subject Index

Absorption 327
Absorption of radiation 289–292, 299, 300
Actinides 244
Aharonov-Bohm effect 142–146
Angular momentum 101–112
– algebraic treatment 391–396
Angular momentum addition 185–193
Angular momentum commutation relations 101
Angular momentum quantization 9–10, 104–106
Angular momentum states 107, 321, 391–396
Antiquark 83
α-rays 101–103
Atomic theory 8–10, 219–249, 327
Average value
(*see also* Expectation value) 15–16, 25, 34, 37, 357

Baker-Hausdorff formula 23
Balmer formula 8
Balmer series 125
Baryon 220, 224
Basis 98
Basis system 164, 376
Bell inequality 379–381, 382
Bessel functions 201, 313, 337
– spherical 304–306, 309, 313–314, 322
Bound state 73–74, 78–79, 116–118, 202, 267, 273, 306, 348, 351
Boundary conditions 59, 70
Bra 159
Breit-Wigner formula 80, 84, 332
Brillouin-Wigner perturbation theory 203

Cathode rays 8
Causality 357–359
Center-of-mass frame 232, 274, 338
Central potential 113–135, 303–314
Centrifugal potential 115–116, 323
Characteristic function 33
Clebsch-Gordan coefficients 191–193
Cold emission 88
Combination principle, Ritz's 124
Commutation relations 27, 44, 353, 391
Commutator 21–22, 27, 44, 344
Compatibility of measurements 99
Complete orthonormal set 31, 40, 160, 360
Complete orthonormal system, *see* Complete orthonormal set
Complete set of observables, *see* Complete set of operators

Eigenfunction 34, 46, 344–346
– radial 321
–– calculation 322–324
EPR argument 377–378
Exchange term 228, 231, 237, 241, 268, 272

f-sum rule 302
Fermi energy 223

H_2^+ molecule 26
Half-life 65
Holzwarth energies 68